STARCH CONSOLIDATION CASTING METHOD FOR PREPARATION OF ZrO$_2$–Al$_2$O$_3$–MgO POROUS STRUCTURE

Rusul Ahmed Shakir (iD)
PhD student, Institute of Polymer and Ceramic Engineering, University of Miskolc
3515 Miskolc, Miskolc-Egyetemváros, e-mail: alshalal.rusul.ahmed.shakir@student.uni-miskolc.hu

Róbert Géber (iD)
associate professor, Institute of Polymer and Ceramic Engineering, University of Miskolc
3515Miskolc, Miskolc-Egyetemváros, e-mail: robert.geber@uni-miskolc.hu

Abstract

The starch consolidation casting (SCC) method was used for the preparation of porous structure ceramic based on partially stabilized ZrO$_2$ with other oxides such as MgO and Al$_2$O$_3$ with the addition of tapioca and potato starch as a binder and pore-forming agents. For casting purpose, three impermeable plastic moulds were designed and manufactured with different sizes and shapes depending on the shape and size of the required samples. The method is based on the fact that after being heated to about 80°C, starch may swell and absorb water from aqueous ceramic solutions. The process's simplicity, the ability to create complicated shapes using different moulds, and the inexpensive cost of the necessary processing tools and materials are its main benefits.

Keywords: Biomedical applications, porous structure, starch consolidation casting, ZrO$_2$

1. Introduction

Oxide ceramic materials have attracted more interesting in various sectors such as in chemical, electrical, biomedical and mechanical engineering due to their unique characteristics such as their biocompatibility, their mechanical properties, and their high chemical resistance (Zhao et al., 2021; Yan et al., 2020). Many studies presented that zirconia-based biomaterial ceramics showed higher resistance to fracture, higher toughness and superior biocompatibility than other ceramic oxides. The main problem of using zirconia-based ceramics is the in vivo ageing associated imperfections as a result of phase transition to monoclinic phase from tetragonal phase when zirconia biomaterials have a direct connection with the body physiological fluids (Nowicka et al., 2020). This transformation, related with a volumetric expansion about 4–5%, contributes to the decrease in zirconia-based ceramics implant strength. Different types of oxides are used as stabilizers (such as Y$_2$O$_3$, MgO and others) to maintain the appropriate tetragonal phase at room temperature (Rodaev et al., 2019).

Porous ceramics are used in a wide range of applications, e.g. thermal insulation (Zhou et al., 2016), filters and membranes (Young et al., 2021), catalyst supports (Vernoux et al., 2009) and biomaterials (Laasri et al., 2010). Based on the application type, various microstructures and preparation methods are needed for porous ceramic bodies. The important criteria in bio-ceramics applications can be open porosity and sufficient pore size (Masters and Anseth, 2004) (e.g. for tissue ingrowth, the minimal pore size aperture is above 100μm, particularly for bone tissue.). The final material properties are determined by the chemical composition and microstructure of the material. Thus, the attainment of required

performance parameters is critically dependent on the possibility of efficiently controlling composition (via batch formulation) and microstructure (via processing).

Pore-forming additives (PFAs) are useful components for the preparation of porous ceramics (Živcová-Vlcková et al., 2012). PFAs have seen an increase in popularity over the past 25 years, and new porous ceramic preparation techniques have also been developed, leading to the adoption of a novel principle known as starch consolidation casting. Starch consolidation casting was designed and for the first time published in the year 1998 by Lyckfeldt and Ferreira (Lyckfeldt and Ferreira, 1998). In this technique, starch acts as a pore-forming component and at the same time as a body-forming agent. Starch is considered a natural biopolymer material and it is perfect for creating porous structures, owing to the low ash percentage that results from starch burnout. Other factors to consider when choosing pore-producing particles include availability, low cost, environmental concerns and combustion products. Starch meets all these characteristics as good as or better than synthetic pore-forming agents (Gregorová et al., 2009; Gregorová et al., 2006). The basis for starch consolidation casting is the capacity of starch to swell by absorbing the water from aqueous ceramic solutions when the system is heated up to approximately 80°C. This temperature-induced swelling and subsequent gelatinization of the starch granules forces the ceramic powder particles into the spaces between the starch granules, converting the ceramic suspension into an elastic ceramic body that may then be dried and fired (Živcová et al., 2010; Rutenberg, 1979).

In this work, starch consolidation casting method was used for the preparation of porous structure ceramic composites. For the purpose of casting process, three impermeable plastic moulds were designed and manufactured with different sizes and shapes depending on the shape and size of the required samples. Porous structure ceramic composites based on partially stabilized zirconia (ZrO$_2$) with other oxides such as magnesia (MgO) and alumina (Al$_2$O$_3$) were prepared utilizing different concentrations of tapioca and potato starch as a pore forming agents.

2. Experimental

2.1. Materials

The following materials were employed in this work: un-stabilized monoclinic zirconia (m-ZrO$_2$) (Interkeram Kft.), magnesia (MgO) (Sigmaaldrich.com, Germany), alumina (AL$_2$O$_3$) (Interkeram Kft.), distilled water, Dolapix CE 64 deflocculant (Zschimmer-Schwarz.com), and potato and tapioca starch as pore-forming agents (Balance food Kft. distributor). The un-stabilized m-ZrO$_2$ was selected in this work as a biomedical material due to its biocompatibility, osteoconductivity, mechanical properties, and chemical inertness. The problem with using pure m-ZrO$_2$ in biomedical applications is its phase instability when the temperature changes, therefore the phase structure is stabilized by the addition of other oxides such as MgO and Al$_2$O$_3$. These oxides are also selected to enhance the biomedical and mechanical properties. Potato and tapioca starches were chosen as pore-forming and body-forming agents, giving the consolidated body strength and allowing de-moulding before drying.

2.2. Sample preparation

2.2.1. Preparation of slurry

The mixing of ceramic powders is the first step in the preparation of the slurry. Different percentages of ceramic powders were mixed utilizing a laboratory milling machine. Ceramic powders were mixed for 5 hours with rotational speed of 60 rpm. Then the mixing process was repeated with the addition of

potato and tapioca starches. The casting slurries were prepared by the fast stirring of the as-prepared powders in distilled water with 1.5 wt% of the deflocculant. Two different solid to liquid ratio slurries were prepared by using a magnetic stirrer and sonication device for 2 hours and at room temperature. The mix compositions that were prepared in this research are listed below in Table 1.

Table 1. *Mix compositions (in wt%)*

m-ZrO$_2$	MgO	Al$_2$O$_3$	Deflocculant	Potato starch	Tapioca starch	Solid phase
77.5	2.5	20	1.5	20	-	70
77.5	2.5	20	1.5	20	-	80
77.5	2.5	20	1.5	-	20	70
77.5	2.5	20	1.5	-	20	80

2.2.2. Preparation of mould

Mould was formed by utilizing 3D printing techniques (Crealty 3D printer, manufactured by Shenzen Creality 3D technology Corporation). Impermeable plastic mould was printed by using HIPS (High Impact Polystyrene) filament. The mould has its own geometry and size depending on the desired shape and size of samples. Figure 1 and Figure 2 show the image for the designed mould.
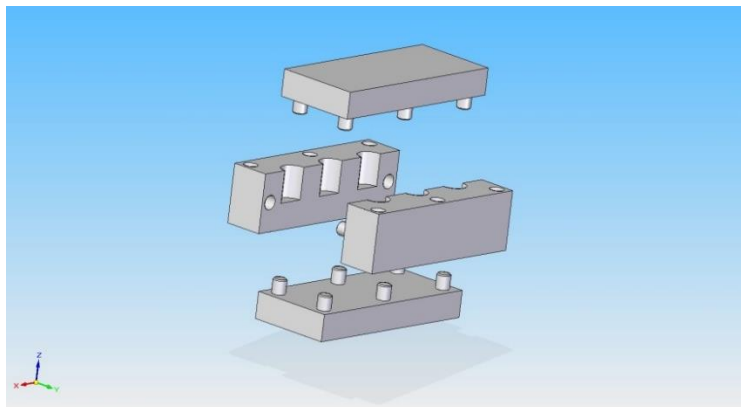

Figure 1. *3D image for the designed mould*

Figure 2. *The 3D printed test mould*

2.2.3. Starch consolidation casting procedures

In the starch consolidation casting method the slurries with different concentrations were poured into the plastic mould. The filled plastic mould was then thoroughly covered with plastic film. This step is very important to avoid the evaporation of water and enables the starch granules to absorb water from the slurry and then swell. The mould with the slurries was put in a laboratory oven (drying oven manufactured by POL-EKO APARATURA) and heated for 2 hours at 80 °C to allow the starch to swell.

2.2.4. Drying

After cooling to room temperature and setting overnight the mould could be opened and the ceramic bodies were de-moulded. After this process, the specimens were dried in a laboratory drier at 60 °C for 2 hours. Figure 3 shows the samples after drying.

Figure 3. *The samples in the mould after drying*

2.3. Characterization method

Microstructural characterization for m-ZrO₂, Al₂O₃ and MgO ceramic powders was carried out using an X-ray diffractometer with Cu Kα radiation in the 2θ range of 3–90°, with a step width of 0.01 and 1 s of exposure time per position. Tapioca starch particle size and shape were observed via utilizing scanning electron microscopy (SEM).

   The particle size distribution of alumina and magnesia ceramic powders was characterized by using CILAS 715 equipment in wet method. The measurements were carried out at room temperature with the addition of two drops of sodium-tripolyphosphate diluted solution as a dispersion agent. The dispersion process was enhanced by the aid of ultrasound for 60 sec. The particle size distributions of m-ZrO₂, tapioca and potato starch powders were determined by using laboratory sieves. The results of sieve analysis are presented in a graph of cumulative percent passing on the Y axis versus the logarithmic sieve size on the X axis.

3. Results and discussion

3.1. X-Ray diffraction

The X-ray diffraction (XRD) technique was used to characterize the phase composition of the raw ceramic powders. The as-received commercial ZrO₂ powder diffraction pattern is shown in Figure 4 As expected; the zirconia powder sample only presents the monoclinic phase zirconia peaks. The results

clearly show that the highest two peaks, which are the (111) and (-111) at 2θ are about 28° and 31°, they are both for monoclinic crystal structure (baddeleyite).
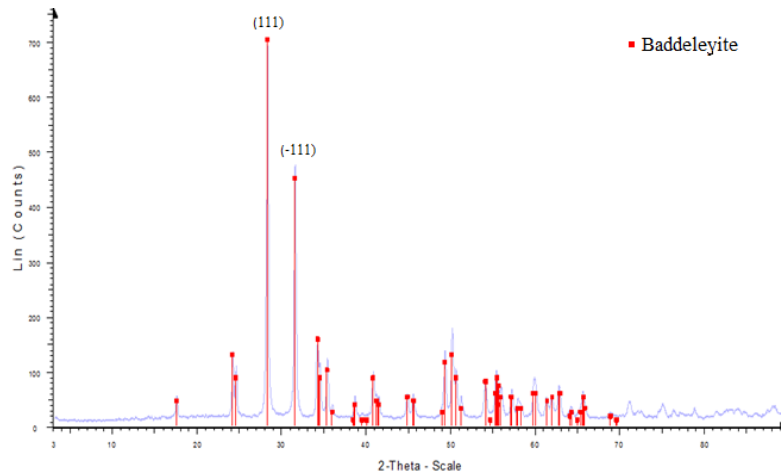

***Figure 4.** XRD spectrum for ZrO₂ powder*

X-ray diffraction spectrum of the alumina powder, as shown in Figure 5, shows that only the pure corundum Al_2O_3 phase was detected with several high intensity peaks at 2θ = 26°, 35°, 38°, 43°, 52°, 57°, 66°, and 68° for planes (012), (104), (110), (113), (024), (116), (216) and (300), respectively.
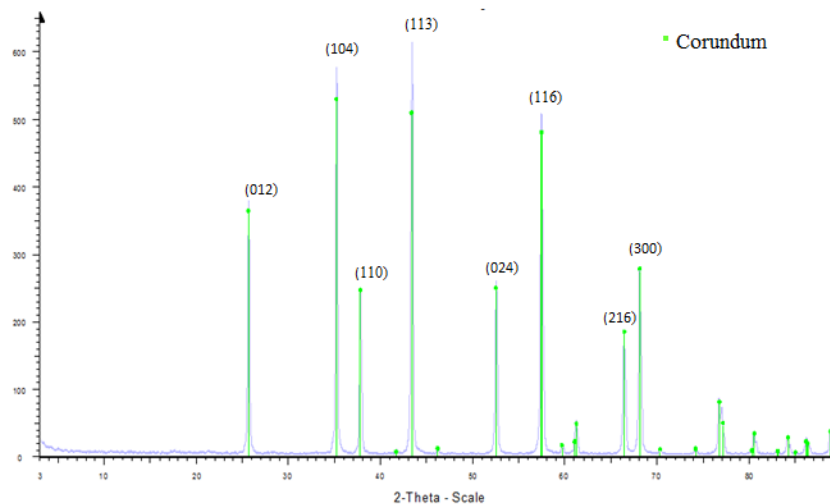
***Figure 5.** XRD spectrum for Al₂O₃ powder*

X-ray diffraction spectrum for MgO powder, shown in Figure 6, shows that the sharper and more intense peaks at diffraction angles of 2θ = 37°, 43°, and 62° are mainly ascribed to diffraction by basal planes (111), (200), (220) of periclase MgO phase, respectively. The result also shows the presence of low intensity peaks for the tridymite SiO_2 phase.
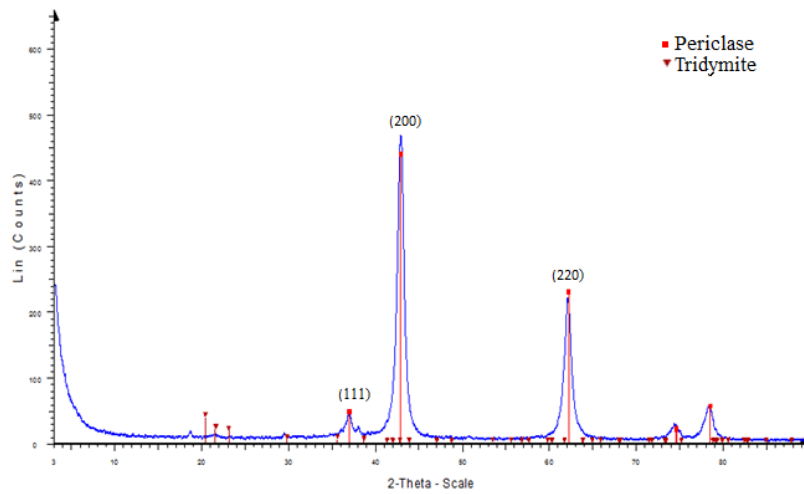
236

Figure 6. *XRD spectrum for MgO powder*

3.2. Scanning electron microscopy (SEM)

The shape, size, and quantity of pore-forming particles have a significant impact on the porous structure that has been generated. In the biomedical application, the shape and size of generated pores must be suitable to facilitate cell migration, proliferation and vascularization. The increased surface area of porous materials, on the other hand, leads to improved bonding with host tissues. As shown in Figure 7, scanning electron microscopy was used to evaluate the tapioca starch particle shape.
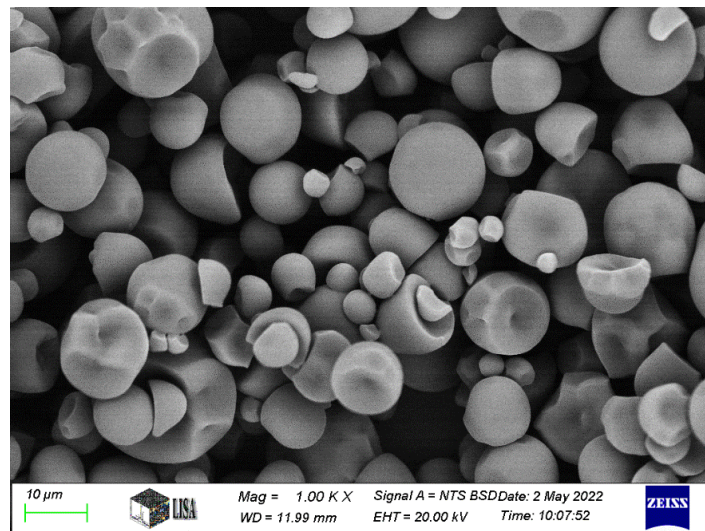

Figure 7. *SEM micrograph for tapioca starch particles*

The SEM *micrograph* shows that the tapioca starch particles present approximately round (spherical) shapes with different particle size distributions. The image shows the presence of particles that are not spherical in shape that is caused by two reasons. The first reason is that these particles are very brittle and may be broken during the preparation of the sample for testing in the SEM laboratory. The second

and more accurate reason is that the particles were broken due to their collision with an electron beam during the test. Figure 8 shows the occurrence of the second cause, as the particle deforms after the examination. Figure (b) shows that there is a crack on the surface of the particle caused after the collision with the electron beam.
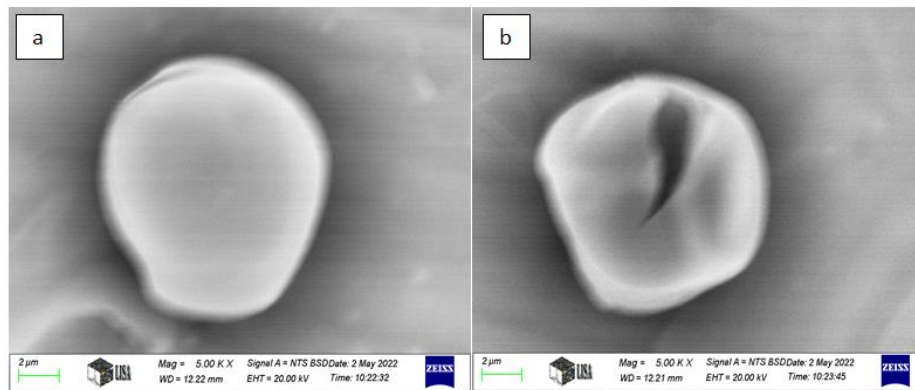

Figure 8. *a) The particle before the electron beam collides;*
b) The particle after the electron beam collides.

3.3. Particle size distribution

A CILAS 715 granulometer was used to determine the particle size distribution of both Al_2O_3 and MgO. As shown in Figure 9, the cumulative percent of particle size distribution for Al_2O_3 are 0.15 μm, 0.57 μm and 1.19 μm for 90% (d_{90}), 50% (d_{50}) and 10% (d_{10}) passing, respectively. In case of MgO powder the cumulative percent are 0.73 μm, 3.99 μm and 9.46 μm for 10%, 50% and 90% passing, respectively.
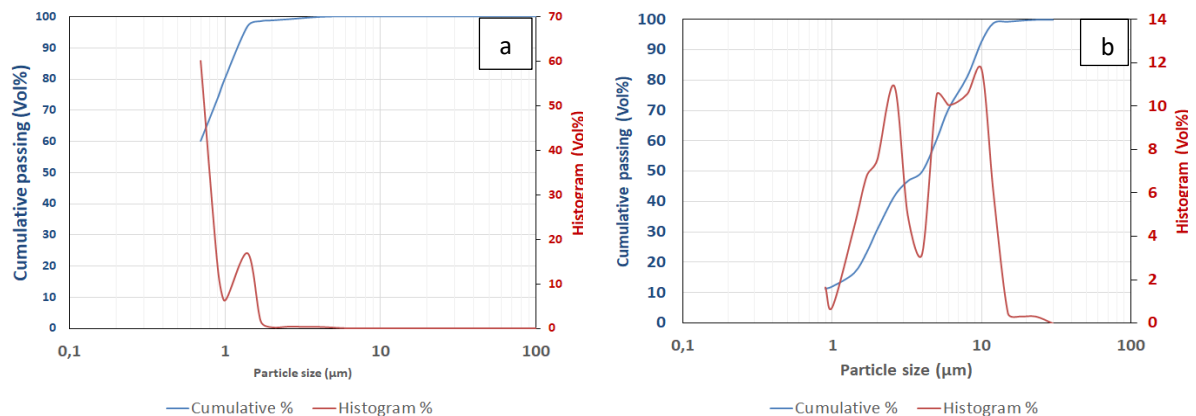

Figure 9. *Particle size distribution for a) Al_2O_3 and b) for MgO*

Laboratory sieves were used to investigate the particle size distribution of m-ZrO₂, tapioca, and potato starch powders. Sieve analysis assumes that all particles will be spherical or nearly round and will pass through the square opening when the particle diameter is less than the size of the square

aperture in the screen. Figure 10 shows the sieve analysis result of zirconium dioxide powder. The values of d_{90}, d_{50} and d_{10} are 96 µm, 86 µm and 59 µm, respectively.
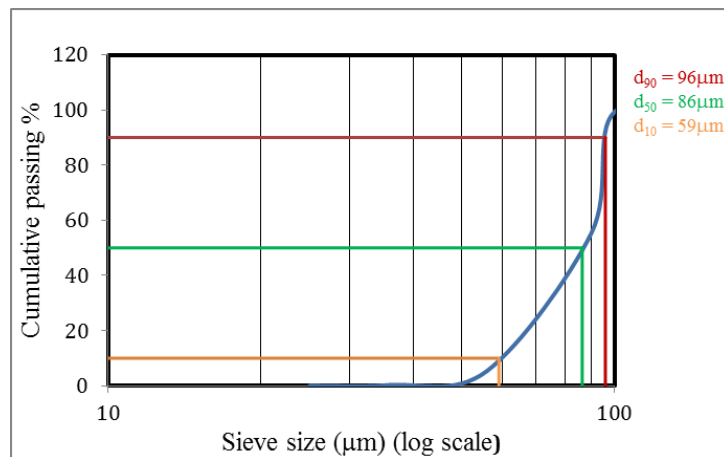

Figure 10. The sieve analysis for ZrO₂ powder

The sieve analysis results of tapioca and potato starches are shown in Figure 11 The particle diameters of tapioca starch are around 78 µm, 48 µm, and 28 µm, while that for potato starch are around 75 µm, 45 µm and 28 µm for 90%, 50% and 10%, respectively.
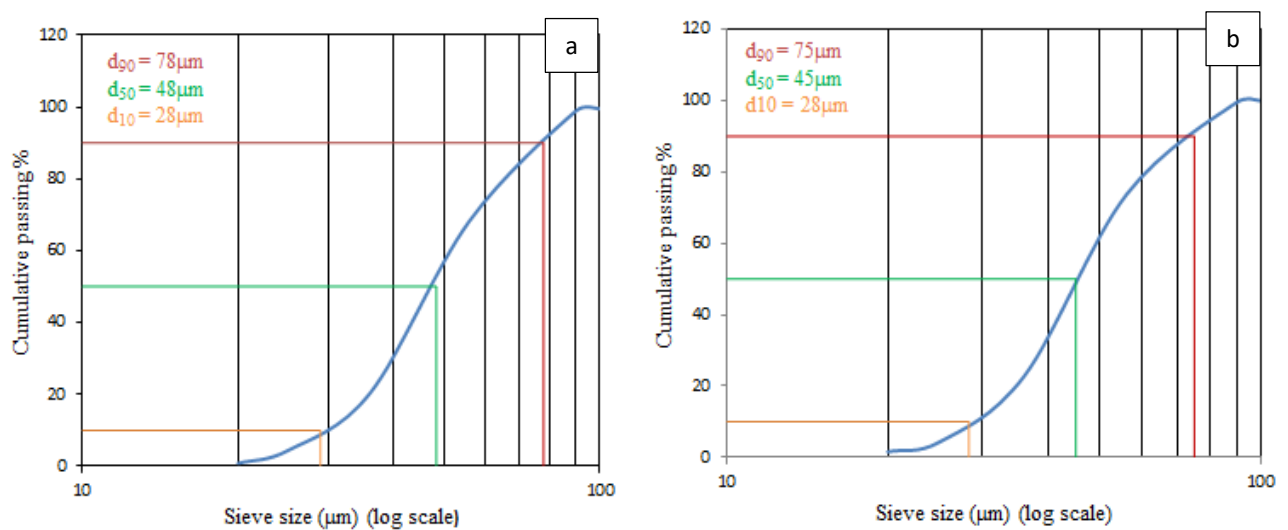

Figure 11. Particle size distribution for a) tapioca starch and b) for potato starch

4. Conclusion

In this work, porous structure ceramics were produced using the starch consolidation casting (SCC) process, which combines partly stabilised ZrO_2 with other oxides including MgO and Al_2O_3, and then uses tapioca and potato starch as binders and pore-forming agents. The conclusions are as following:

1. The X-ray diffraction results show that the used raw materials have pure crystalline structure of baddeleyite of ZrO_2, corundum for Al_2O_3 and periclase with the presence of low intensity peaks for the tridymite SiO_2 phase for MgO.
2. Sieve analysis and the particle size distribution results show that the 50% of particles were in size about 86 μm for ZrO_2, 0.57 μm for Al_2O_3, 3.99 μm for MgO, 48 μm and 45μm for tapioca and potato starches, respectively.
3. Tapioca starch particle size and shape was done via utilizing scanning electron microscopy (SEM) and the results show that the starch has a like spherical shape.
4. Three impermeable plastic moulds were designed and manufactured with different sizes and shapes depending on the shape and size of the required samples.

5. Acknowledgment

References

[1]   Zhao, L., Jiang, Z., & Zhang, C. (2021). Residual stress and fracture toughness of sintered body of ZrO_2-GO composite ceramics material. *Ceramic International*, 47(1), 388–392. **https://doi.org/10.1016/j.ceramint.2020.08.144**

[2]   Yan, S., He, P., Jia, D., Zhuang, K., Duan, X., Wang, S., & Zhou, Y. (2020). Realizing high ceramic yield and low shrinkage of in-situ formed lightweight 3D-SiC (rGO)px polymer-derived ceramics with excellent fracture toughness. *Ceramic International*, 46(17), 27426–27436. **https://doi.org/10.1016/j.ceramint.2020.07.229**

[3]   Nowicka, A., El-Maghraby, H. F., Švančárková, A., Galusková, D., Reveron, H., Gremillard, L., Chevalier, J. & Galusek, D. (2020). Corrosion and low temperature degradation of 3Y-TZP dental ceramics under acidic conditions. *Journal of European ceramic society*, 40(15), 6114–6122. **https://doi.org/10.1016/j.jeurceramsoc.2020.06.019**

[4]   Rodaev, V. V., Razlivalova, S. S., Tyurin, A. I., Zhigachev, A. O., & Golovinet, Y. I. (2019). Microstructure and phase composition of yttria-stabilized zirconia nanofibers prepared by high-temperature calcination of electrospun zirconium acetylacetonate/yttrium nitrate/polyacrylonitrile fibers. *Fibers*, 7(10), 82. **https://doi.org/10.3390/fib7100082**

[5]   Zhou, W., Zhang, R., Fang, D. (2016). Design and analysis of the porous ZrO_2/(ZrO_2+Ni) ceramic joint with load bearing–heat insulation integration. *Ceramics international,* 42(1), part B, 1416–1424. **https://doi.org/10.1016/j.ceramint.2015.09.085**

[6]   Young, C., Zhang, Y. C., Nisar, A., Boesl, B., & Agarwa, A. (2021). Spark plasma sintered porous aluminum oxide for filtration applications. *Ceramics International*, 47(15), 21822–21827. **https://doi.org/10.1016/j.ceramint.2021.04.199**

[7]   Vernoux, P., Guth, M., Li, X. (2009). Ionically conducting ceramics as alternative catalyst supports. *Electrochem Solid-State Lett.,* 12, 9–11. **https://doi.org/10.1149/1.3122746**

[8]   Laasri, S., Taha, M., Laghzizil, A., Hlil, E. K., & Chevalier, J. (2010). The effect of densification and dehydroxylation on the mechanical properties of stoichiometric hydroxyapatite bioceramics. *Mater. Res. Bull.*, 45, 1433–1437. **https://doi.org/10.1016/j.materresbull.2010.06.040**

[9]   Masters, K. S. & Anseth, K. S. (2004). Cell–material interactions. *Adv. Chem. Eng.,* 29, 7–46. **https://doi.org/10.1016/S0065-2377(03)29002-5**

[10]   Živcová-Vlcková, Z., Locs, J., Keuper, M., Sedlárová, I., & Chmelícková, M. (2012). Microstructural comparison of porous oxide ceramics from the system Al$_2$O$_3$–ZrO$_2$ prepared with starch as a pore-forming agent. *Journal of the European Ceramic Society*, 32(10), 2163–2172. **https://doi.org/10.1016/j.jeurceramsoc.2012.02.005**

[11]   Lyckfeldt, O., Ferreira, J. M. F. (1998). Processing of porous ceramics by 'starch consolidation'. *J. Eur. Ceram. Soc.,* 18(2), 131–140. **https://doi.org/10.1016/S0955-2219(97)00101-5**

[12]   Gregorová, E., Živcová, Z., Pabst, W. (2009). Porous ceramics made using potato starch as a pore-forming agent. *Fruit, Vegetable and Cereal Science and Biotechnology,* 3, 115–127.

[13]   Gregorová, E., Živcová, Z., Pabst, W. (2006). Porosity and pore space characteristics of starch-processed porous ceramics. *J. Mater. Sci.,* 41, 6119–6122. **https://doi.org/10.1007/s10853-006-0475-z**

[14]   Živcová, Z., Gregorová, E., Pabst, W. (2010). Low- and high-temperature processes and mechanisms in the preparation of porous ceramics via starch consolidation castin. *Starch/Stärke,* 62, 3–10. **https://doi.org/10.1002/star.200900139**

[15]   Rutenberg, M. W. (1979). Starch and its modifications. In R. L. Davidsson (Ed.), *Handbook of Water-Soluble Gums and Resins* (pp 22: l-83). McGraw-Hill, New York.